NACA

RESEARCH MEMORANDUM

ALTITUDE PERFORMANCE CHARACTERISTICS OF TAIL-PIPE

BURNER WITH CONVERGING CONICAL BURNER

SECTION ON J47 TURBOJET ENGINE

By William R. Prince and John E. McAulay

Lewis Flight Propulsion Laboratory
Cleveland, Ohio

NATIONAL ADVISORY COMMITTEE
FOR AERONAUTICS

WASHINGTON
December 19, 1950

NATIONAL ADVISORY COMMITTEE FOR AERONAUTICS

RESEARCH MEMORANDUM

ALTITUDE PERFORMANCE CHARACTERISTICS OF TAIL-PIPE

BURNER WITH CONVERGING CONICAL BURNER

SECTION ON J47 TURBOJET ENGINE

By William R. Prince and John E. McAulay

SUMMARY

An investigation of turbojet-engine thrust augmentation by means of tail-pipe burning was conducted in the NACA Lewis altitude wind tunnel. Performance data were obtained with a tail-pipe burner having a converging conical burner section installed on an axial-flow-compressor type turbojet engine over a range of simulated flight conditions and tail-pipe fuel-air ratios with a fixed-area exhaust nozzle.

A maximum tail-pipe combustion efficiency of 0.86 was obtained at an altitude of 15,000 feet and a flight Mach number of 0.23. At an altitude of 25,000 feet, a tail-pipe burner-inlet temperature of 1700° R, and rated engine speed, the ratio of augmented thrust to normal thrust increased from 1.3 at a flight Mach number of 0.23 to 1.4 at a flight Mach number of 0.76. Tail-pipe burner operation was possible up to an altitude of 45,000 feet at a flight Mach number of 0.23.

INTRODUCTION

An extensive research program on thrust augmentation of turbojet engines has been conducted in the NACA Lewis altitude wind tunnel to determine the effect of various component designs on the performance and operational characteristics of several tail-pipe burner installations. The effect of flame-holder and fuel-system design on the burner performance and the effect of altitude and flight Mach number on over-all performance with a fixed-area exhaust nozzle are reported in references 1 to 4. Altitude performance characteristics of a tail-pipe burner having a converging conical burner section are presented in this report.

1372

Performance data were obtained with the converging-burner configuration installed on a J47 turbojet engine over a range of simulated flight conditions and tail-pipe fuel-air ratios with a fixed-area exhaust nozzle. The tail-pipe burner was designed for use in a particular airplane. The fuselage dimensions limited the maximum diameter of the burner and necessitated the use of a converging combustion chamber. The burner configuration discussed in this report is a modified version of a tail-pipe burner whose performance is reported in reference 2. This modification resulted from the greater air flow of the J47 turbojet engine used in this investigation as compared with the J35 engine (reference 2). Because of the increased air flow, it was necessary to fabricate a larger burner to reduce the burner-inlet velocity and burner total-pressure loss. The modified burner had the largest diameter that could be used without making major changes in the airplane fuselage. This final configuration incorporated the best flame holder and fuel system previously determined from the investigation reported in reference 2.

Tail-pipe burner performance at several flight conditions is given in both tabular and graphical forms and compared with performance of the standard engine and of the tail-pipe burner reported in reference 2.

APPARATUS AND INSTRUMENTATION

Engine

Tail-pipe burner performance was investigated using a J47 turbojet engine having a static sea-level thrust rating of 5000 pounds at an engine speed of 7900 rpm and a turbine-outlet temperature of 1275° F (1735° R). The air flow is approximately 94 pounds per second at static sea-level rated conditions. The principal components of this engine are a 12-stage axial-flow compressor, eight cylindrical through-flow combustion chambers, a single-stage turbine, and a tail pipe. The over-all length of the engine with standard tail pipe is 143 inches and the maximum diameter is 37 inches. The length of the standard-engine tail pipe is 35 inches. A fixed-area exhaust nozzle with which rated conditions were obtained had an outlet area of 280 square inches.

Installation

The engine and tail-pipe burner were mounted on a wing section that spanned the 20-foot-diameter test section of the Lewis altitude

1372

wind tunnel (fig. 1). For this investigation the standard-engine tail-pipe was replaced by a tail-pipe burner assembly which was attached to the downstream flange of the turbine casing. In order to provide accessibility for instrumentation, no cowling was installed around the engine.

Air entered the engine inlet through a duct from the tunnel make-up air system. This duct was connected to the engine inlet by means of a slip joint with a frictionless seal so that thrust and drag could be measured by the balance scales.

Tail-Pipe Burner

The tail-pipe burner was designed by the manufacturer in conformance with the available space in the airplane. A cross-sectional view showing the dimensions of the tail-pipe burner is shown in figure 2. The three main sections of the tail-pipe burner assembly are the diffuser section, the combustion chamber, and the nozzle section, as shown in figure 3. A fixed conical exhaust nozzle was used for the entire investigation inasmuch as a variable-area nozzle was not available for this burner. Cooling liners, providing a 1/2-inch radial space between the liner and the burner shell and extending the full length of the tail-pipe combustion chamber, were installed in a manner similar to that discussed in reference 1.

The minimum diffuser diameter, which occurred at the downstream end of the diffuser inner body, was 25 inches and the maximum diameter in the combustion chamber was $31\frac{1}{2}$ inches. The diameter of the conical exhaust nozzle was $25\frac{3}{32}$ inches, which gave a fixed area of 494 square inches, and the tail-pipe burner length including the exhaust nozzle was $138\frac{3}{4}$ inches. A typical two-annular V-type flame holder used throughout the investigation is shown in figure 4. The flame holder, which was mounted $2\frac{3}{4}$ inches downstream of the combustion-chamber inlet, had outer and inner ring diameters of 23 inches and 14 inches, respectively, and blocked 31.5 percent of the burner cross-sectional area.

Fuel was injected at two stations into the burner normal to the direction of gas flow (fig. 5). At the upstream station, fuel was injected from 12 tubes $1\frac{3}{16}$ inches long extending from the diffuser inner cone and located about 44 inches upstream of the flame holder.

Each tube had two 0.031-inch-diameter holes. At the downstream sta-
tion, fuel was injected from two sets of different length radial
spray tubes $18\frac{1}{2}$ inches upstream of the flame holder. One set con-
sisted of six fuel tubes $8\frac{1}{2}$ inches long with six 0.041-inch-diameter
holes per tube and the other of six tubes $7\frac{5}{16}$ inches long with four
0.031-inch-diameter holes per tube. Rate of fuel injection from the
three sets of spray tubes was determined by a flow divider installed
in the tail-pipe fuel system as shown in figure 5. The fuel-flow
schedule provided by the flow divider is shown in figure 6. At low
tail-pipe fuel flows, approximately 60 percent of the tail-pipe fuel
was injected through only the primary system which consisted of the
six short tubes and the 12 spray tubes on the inner cone ring. The
remaining fuel was injected through the six long tubes.

Ignition of the tail-pipe fuel was accomplished by either of
two systems. For one ignition system, fuel was injected through a
30-gallon-per-hour spray nozzle installed in the center of the dif-
fuser inner cone. Ignition of this fuel was obtained by two spark
plugs inserted in the pilot cone (fig. 3). The other system pro-
vided ignition by a momentary increase in fuel flow to the fuel
nozzle in one of the engine combustors. This excess fuel in one
engine combustor resulted in a burst of flame through the turbine,
thereby igniting the tail-pipe fuel. With this system of igni-
tion, the cone fuel also had to be on to carry the flame back to
the flame holder.

Instrumentation

Instrumentation was installed at the engine inlet to measure
engine air flow and in the tail-pipe to measure the burner per-
formance. Location of the instrumentation in the tail-pipe burner
is shown in figure 3, and cross sections of instrumentation at
stations 6 and 8 are shown in figure 7. The instrumentation at
station 7 consisted of four static wall orifices approximately
9 inches upstream of the flame holder. The exhaust-nozzle rake
installed at station 8 was water cooled.

PROCEDURE

Data were obtained over a range of altitudes from 15,000 to
45,000 feet for a range of flight Mach numbers from 0.22 to 0.76.
At each flight condition, performance data were obtained for

1372

several tail-pipe fuel flows between the lean combustion blow-out limit and the fuel flow required for limiting turbine-outlet temperature. All tail-pipe burning data were obtained at rated engine speed (7900 rpm).

Dry refrigerated air was supplied to the engine from the tunnel make-up air system at the standard temperature for each flight condition, except that the minimum temperature obtained was about -20° F. The air was throttled from approximately sea-level pressure to the desired total pressure at the engine inlet. Complete free-stream ram-pressure recovery was assumed at each flight condition in the calculation of flight Mach number.

Thrust measurements were obtained from the tunnel balance scales and from the tail-rake pressure survey at the exhaust nozzle. The thrust values presented were obtained from the balance-scale measurements. The thrust obtained from tail-rake measurements was used in determining exhaust-gas temperature and combustion efficiency. Methods of obtaining the important tail-pipe burner parameters and the symbols used are given in the appendix.

The fuel used in the engine was AN-F-32 kerosene having a lower heating value of 18,550 Btu per pound and a hydrogen-carbon ratio of 0.155. Fuel used in the tail-pipe burner was AN-F-48b, grade 80, gasoline having a lower heating value of 19,000 Btu per pound and a hydrogen-carbon ratio of 0.186.

RESULTS AND DISCUSSION

As a preliminary phase of this investigation, a smaller diameter tail-pipe burner having a converging burner section similar in shape to the one discussed in this report was investigated on a J47 turbojet engine. Unpublished results showed that tail-pipe burner operation was unsatisfactory at rated engine speed because of the high combustion-chamber-inlet velocities. The combustion-chamber-inlet velocities under these conditions were in the order of 700 feet per second. In order to reduce this velocity, the tail-pipe burner diameters were increased approximately 3 inches. This increase in diameter was the largest that could be used without making major changes to the airplane fuselage. As a result of this enlargement of the burner, the combustion-chamber-inlet velocity was reduced approximately 20 percent. Results of the investigation of this larger burner are presented graphically to show the effect of altitude and flight Mach number on the significant burner-performance characteristics. All data for this investigation are also presented in table I.

1372

Burner Performance Characteristics

Effect of altitude. - The effect of altitude on burner per-
formance is shown in figures 8 to 10 for a flight Mach number of
0.23 and at rated engine speed. The variation of combustion-
chamber-inlet velocity and tail-pipe burner-inlet conditions with
tail-pipe fuel-air ratio is shown in figure 8. The tail-pipe fuel-
air ratio is defined as the ratio of tail-pipe fuel flow to the
unburned air flow entering the tail-pipe. For the range of tail-
pipe fuel-air ratios, increasing the altitude from 15,000 to
45,000 feet had little effect on the combustion-chamber-inlet veloc-
ity and the tail-pipe burner-inlet temperature. The turbine-outlet
total pressure was reduced approximately in proportion to the reduc-
tion in compressor-inlet pressure. For the entire range of alti-
tudes investigated, the combustion-chamber-inlet velocity varied
between 525 and 575 feet per second.

The effect of altitude on the variation of exhaust-gas total
temperature and tail-pipe combustion efficiency with tail-pipe
fuel-air ratio is shown in figure 9. Maximum combustion efficiency
was reduced from 0.86 to 0.80 as the altitude was increased from
15,000 to 35,000 feet. Further increase in altitude greatly reduced
the combustion efficiency. The maximum combustion efficiency
occurred at tail-pipe fuel-air ratios between approximately 0.040
and 0.050.

The exhaust-nozzle-outlet temperature, over the range of tail-
pipe fuel-air ratios investigated, was reduced about 600° R with
increase in altitude from 15,000 to 45,000 feet, with the greater
portion of this decrease occurring at an altitude above 35,000 feet.
This decrease in exhaust-gas temperature is a result of a change in
engine characteristics with a change in Reynolds number. With an
increase in altitude, the Reynolds number effect on the compressor
(reference 5) caused a decrease in compressor efficiency which
necessitated increasing the exhaust-nozzle area in order to obtain
rated engine conditions at limiting turbine-outlet temperature.
Consequently, because the data presented herein are for a fixed-
area exhaust nozzle, the available exhaust-gas temperature with
afterburning is considerably lower at 45,000 feet than at 15,000 feet.
For optimum performance the nozzle area should be adjusted by use of
a variable-area nozzle so that the pressures and temperatures at the
turbine outlet are the same with the afterburner operative or
inoperative.

Variation of the over-all burner performance characteristics
with altitude at a tail-pipe burner-inlet temperature of 1700° R

1372

and rated engine speed is shown in figure 10. These results were obtained by cross-plotting and in some cases by slight extrapolation of jet thrust and total fuel flow at a constant tail-pipe burner-inlet temperature of 1700° R.

Thrust-augmentation characteristics are presented in terms of the augmented thrust ratio, which is defined as the ratio of augmented thrust to normal thrust as defined in the appendix. For altitudes up to 25,000 feet, the augmented thrust ratio was 1.30 and then decreased to 1.13 as the altitude increased to 45,000 feet. The total-pressure loss across the standard-engine tail pipe was 0.032 of the tail-pipe burner-inlet total pressure for all flight conditions at rated engine speed. This value was obtained during previous operation of the engine with a fixed-conical exhaust nozzle. With the tail-pipe burner installed but inoperative, this value increased from 0.052 to 0.071 as the altitude was increased from 15,000 to 45,000 feet at a flight Mach number of 0.23. As a result of this greater pressure loss across the tail-pipe burner, the augmented thrust ratio with tail-pipe burner inoperative was 0.98 at 15,000 feet and decreased to 0.96 at 45,000 feet.

The specific fuel consumption of the standard engine based on net thrust increased from 1.15 to 1.25 as the altitude was raised from 15,000 to 45,000 feet. With tail-pipe burning, the specific fuel consumption was 2.95 at 15,000 feet and 3.40 at 45,000 feet. This expected increase in specific fuel consumption with increase in altitude resulted from the lower tail-pipe combustion efficiency at higher altitudes.

Effect of flight Mach number. - The effect of flight Mach number on burner performance is shown in figures 11 to 13 for an altitude of 25,000 feet and rated engine speed. The variation of combustion-chamber-inlet velocity and tail-pipe burner-inlet conditions with tail-pipe fuel-air ratio is shown in figure 11 for several flight Mach numbers. At a given tail-pipe fuel-air ratio, increasing the flight Mach number from 0.23 to 0.76 had no effect on the combustion-chamber-inlet velocity. At tail-pipe burner-inlet temperatures above 1500° R, the combustion-chamber-inlet velocity was about 525 feet per second for all flight Mach numbers investigated. Variations of flight Mach number, over the range investigated, had little effect on tail-pipe burner-inlet temperature. The tail-pipe burner-inlet temperature was approximately 50° R higher at a given tail-pipe fuel-air ratio for a flight Mach number of 0.23 than for the two higher flight Mach numbers investigated. The tail-pipe burner-inlet pressure increased approximately in proportion to the compressor-inlet pressure.

1372

The effect of flight Mach number on variation of exhaust-gas total temperature and tail-pipe combustion efficiency with tail-pipe fuel-air ratio is shown in figure 12. Peak tail-pipe combustion efficiencies of 0.82 at a flight Mach number of 0.23, and 0.84 at flight Mach numbers of 0.54 and 0.76 were obtained at a tail-pipe fuel-air ratio of approximately 0.043. Exhaust-gas total temperature was unaffected by changes in flight Mach number and increased to a maximum value of 3480° R as the tail-pipe fuel-air ratio was raised to 0.0625.

Variation of the over-all burner performance characteristics with flight Mach number at a tail-pipe burner-inlet temperature of 1700° R and at rated engine speed is shown in figure 13. These results were obtained by cross-plotting and extrapolating in a manner similar to that previously mentioned. The augmented thrust ratio increased from 1.29 at a flight Mach number of 0.23 to 1.4 at a flight Mach number of 0.76. This curve indicates that further increases in flight Mach number would have a very small effect on augmented thrust ratio. The tail-pipe total-pressure loss with the tail-pipe burner installed, but inoperative, was 0.058 of the tail-pipe burner-inlet total pressure and the augmented thrust ratio was about 0.98 for all flight Mach numbers investigated.

The specific fuel consumption based on net thrust of the standard engine was approximately 1.2 for all flight Mach numbers investigated. With tail-pipe burning, the specific fuel consumption was 2.95 at a flight Mach number of 0.23. Increasing the Mach number to 0.54 raised this value to 3.30 and a further increase in Mach number to 0.76 lowered the specific fuel consumption to 2.98.

Performance characteristic curves for a converging-conical tail-pipe burner on a J35 turbojet engine are also shown on figure 13. These data are not directly comparative inasmuch as they are for a lower tail-pipe burner-inlet total temperature (1650° R) and a smaller exhaust-nozzle outlet area (296 square inches) than for the data obtained with the J47 engine. The curves are presented, however, to indicate the relative performance of two converging-conical burners on two different turbojet engines. The augmented thrust ratio for the burner on the J35 engine is 10 to 15 percent higher and the specific fuel consumption is about 25 percent lower than for the burner on the J47 engine. The augmented thrust ratio was lower for the burner used on the J47 engine than for the burner used on the J35 engine, probably because of the greater tail-pipe total-pressure loss ratio. At the operating conditions shown in figure 13, the pressure loss was about 0.15 of the tail-pipe burner-inlet total pressure for the burner used on the J47 engine as compared with 0.085 in the J35 tail-pipe burner.

1372

Burner Operational Characteristics

Two methods were used to ignite the tail-pipe fuel. The first method utilized the pilot cone at the downstream end of the diffuser inner body to provide a sheltered region in which to install a fuel nozzle and spark plugs. Fuel was supplied to the ignition region by the nozzle in the pilot cone and by the fuel-spray tubes on the diffuser inner cone. This system gave successful starts only at altitudes below 20,000 feet and reduced engine speed. When fuel was supplied to the nozzle in the pilot cone at rated engine speed, the flame holder appeared very hot.

In the second method employed, fuel was momentarily injected into one of the engine combustors with a resultant burst of flame through the turbine and into the tail-pipe. This method provided satisfactory ignition of the tail-pipe fuel up to an altitude of 45,000 feet at rated engine speed and a flight Mach number of 0.23. Successful burner operation was also possible at these conditions.

The use of an internal cooling liner extending the full length of the combustion chamber having a 1/2-inch gap between the liner and the burner shell provided adequate shell cooling at all flight conditions investigated.

SUMMARY OF RESULTS

As a preliminary phase of this investigation, a smaller diameter tail-pipe burner having a converging burner section similar in shape to the one discussed in this report was investigated, and the results indicated that tail-pipe burner performance was unsatisfactory with combustion-chamber-inlet velocities in the order of 700 feet per second. Satisfactory performance was obtained with an enlarged burner in which the combustion-chamber-inlet velocities were approximately 550 feet per second.

The following results were obtained from an investigation of the enlarged tail-pipe burner having a converging burner section and a fixed-area exhaust nozzle on a J47 turbojet engine in the NACA Lewis altitude wind tunnel:

1. A maximum tail-pipe combustion efficiency of 0.86 was obtained at an altitude of 15,000 feet, a flight Mach number of 0.23, and a tail-pipe fuel-air ratio of 0.040.

2. At an altitude of 25,000 feet, a tail-pipe burner-inlet temperature of 1700° R, rated engine speed, and flight Mach numbers from 0.23 to 0.76, the ratio of augmented thrust to normal thrust increased from 1.3 to 1.4 and the specific fuel consumption based on net thrust of the standard engine varied from 3.0 to 3.3.

3. Tail-pipe burner operation was possible up to an altitude of 45,000 feet at a flight Mach number of 0.23.

Lewis Flight Propulsion Laboratory,
    National Advisory Committee for Aeronautics,
        Cleveland, Ohio.

APPENDIX - CALCULATIONS

Symbols

1372

The following symbols are used in the calculations and on the figures:

A   cross-sectional area, sq ft

B   thrust scale reading, lb

C_j jet velocity coefficient, ratio of scale jet thrust to rake
            jet thrust

C_T thermal-expansion ratio, ratio of hot exhaust-nozzle area
            to cold exhaust-nozzle area

D   external drag of installation, lb

D_r drag of exhaust-nozzle survey rake, lb

F_j jet thrust, lb

F_n net thrust, lb

f/a   fuel-air ratio

g   acceleration due to gravity, 32.2 ft/sec^2

H   total enthalpy, Btu/lb

h_c lower heating value of fuel, Btu/lb

M   Mach number

P   total pressure, lb/sq ft absolute

P_8' total pressure at exhaust-nozzle survey station in standard-
            engine tail pipe, lb/sq ft absolute

p   static pressure, lb/sq ft absolute

R   gas constant, 53.4 ft-lb/(lb)(^{O}R)

T   total temperature, ^{O}R

t	static temperature, °R
V	velocity, ft/sec
W_a	air flow, lb/sec
W_c	compressor leakage air flow, lb/sec
W_f	fuel flow, lb/hr
W_g	gas flow, lb/sec
W_f/F_n	specific fuel consumption based on total fuel flow and net thrust, lb/(hr)(lb thrust)
γ	ratio of specific heats for gases
η_b	combustion efficiency

Subscripts:

a	air
e	engine
f	fuel
i	indicated
j	jet
m	fuel manifold
s	scale
t	tail-pipe burner
x	inlet duct at frictionless slip joint
0	free-stream conditions
1	engine inlet
6	tail-pipe burner inlet (turbine outlet)

1372

7   tail-pipe combustion-chamber inlet

8   exhaust nozzle, 1 inch upstream of fixed portion of
         exhaust-nozzle outlet

9   exhaust-nozzle outlet

Methods of Calculation

Flight Mach number and airspeed. - Flight Mach number and
equivalent airspeed were calculated from ram-pressure ratio by
the following equations assuming complete pressure recovery at
the engine inlet:

$$M_0 = \sqrt{\frac{2}{\gamma_1 - 1}\left[\left(\frac{P_1}{p_0}\right)^{\frac{\gamma_1 - 1}{\gamma_1}} - 1\right]} \qquad (1)$$

$$V_0 = M_0 \sqrt{\gamma_1 g R T_1 \left(\frac{p_0}{P_1}\right)^{\frac{\gamma_1 - 1}{\gamma_1}}} \qquad (2)$$

Air flow. - Air flow at the engine inlet was determined from
pressure and temperature measurements obtained with four survey
rakes in the inlet annulus. The following equation was used to
calculate air flow:

$$W_{a,1} = p_1 A_1 \sqrt{\frac{2\gamma_1 g}{(\gamma_1 - 1)R t_1}\left[\left(\frac{P_1}{p_1}\right)^{\frac{\gamma_1 - 1}{\gamma_1}} - 1\right]} \qquad (3)$$

Air flow at station 6 was obtained by taking into account the
measured air leakage at the last stage of the compressor in the
following manner:

$$W_{a,6} = W_{a,1} - W_c \qquad (4)$$

Temperatures. - Static temperature was calculated from indicated temperature, using an impact recovery factor of 0.85.

$$t = \frac{T_1}{1 + 0.85\left[\left(\frac{P}{p}\right)^{\frac{\gamma-1}{\gamma}} - 1\right]} \tag{5}$$

Total temperature was calculated by the adiabatic relation between temperatures and pressures.

Gas flow. - The total weight flow was calculated as follows:

$$\text{(Engine)} \quad W_{g,6} = W_{a,6} + \frac{W_{f,e}}{3600} \tag{6}$$

$$\text{(Tail pipe)} \quad W_{g,7} = W_{g,8} = W_{a,6} + \frac{W_{f,e} + W_{f,t}}{3600}$$

Tail-pipe combustion-chamber-inlet velocity. - Velocity at the combustion-chamber inlet during burning was calculated from the continuity equation using static pressure measured at station 7, approximately 9 inches upstream of the flame holder, and assuming constant total pressure and total temperature from the tail-pipe burner inlet to the combustion-chamber inlet

$$V_7 = \frac{W_{g,7} R T_6}{p_7 A_7}\left(\frac{p_7}{P_6}\right)^{\frac{\gamma_6 - 1}{\gamma_6}} \tag{7}$$

Tail-pipe fuel-air ratio. - The tail-pipe fuel-air ratio is defined as the ratio of the weight flow of fuel injected in the tail-pipe burner to the weight flow of unburned air entering the tail-pipe burner from the engine. Weight flow of unburned air was determined by assuming the fuel injected in the engine combustor was completely burned therein.

$$(f/a)_t = \frac{W_{f,t}}{3600(W_{a,6}) - \frac{W_{f,e}}{0.068}} \tag{8}$$

where 0.068 is the stoichiometric fuel-air ratio for the engine fuel.

1372

The total fuel-air ratio for the engine and tail-pipe burner is:

$$(f/a) = \frac{W_{f,e} + W_{f,t}}{3600 \; W_{a,6}} \qquad (9)$$

Combustion efficiency. - Tail-pipe combustion efficiency was obtained by dividing the enthalpy rise through the tail-pipe burner by the product of the tail-pipe fuel flow and the lower heating value of the tail-pipe fuel, disregarding dissociation of the exhaust gas.

$$\eta_{b,t} = \frac{3600 \; W_g \Delta H_t}{W_{f,t} \; h_{c,t}}$$

$$\qquad (10)$$

$$= \frac{3600(W_{a,6})H_a\Big]_{T_1}^{T_8} + W_{f,e}H_{f,e}\Big]_{T_m}^{T_8} + W_{f,t}H_{f,t}\Big]_{T_m}^{T_8} - W_{f,e}h_{c,e}}{W_{f,t} \; h_{c,t}}$$

The engine fuel was assumed to be completely burned in the engine; inasmuch as the engine combustion efficiency has been found to be about 98 percent at rated engine speed, this assumption involves an error in tail-pipe combustion efficiency of less than 0.5 percent. The enthalpy of the products of combustion was obtained from a chart using the hydrogen-carbon ratio and the temperature. This method is explained in reference 5.

Augmented thrust. - Scale jet thrust was determined from the balance-scale measurements by use of the following equation:

$$F_{j,s} = B + D + D_r + \frac{W_{a,x}V_x}{g} + A_x \; (p_x-p_0) \qquad (11)$$

The last two terms of this expression represent the momentum and pressure forces on the installation at the slip joint in the inlet-air duct. The external drag of the installation was determined with the engine inoperative and with a blind flange installed in the engine inlet to prevent air flow through the engine. Drag of the exhaust-nozzle survey rake was measured over a range of jet Mach numbers by a hydraulic balance piston mechanism.

Scale net thrust was obtained by subtracting the equivalent free-stream momentum of the inlet air from the scale jet thrust

$$F_{n,s} = F_{j,s} - \frac{W_{a,1} V_0}{g}$$ (12)

Rake thrust is given by the following equation based on pressure obtained at station 8:

$$F_{j,8} = \frac{2C_T A_8 p_8 \gamma_9}{\gamma_9 - 1}\left[\left(\frac{P_8}{p_8}\right)^{\frac{\gamma_9 - 1}{\gamma_9}} - 1\right] + A_8 C_T (p_8 - p_0)$$ (13)

The value of γ_9 was obtained from an approximate exhaust-nozzle-outlet temperature calculated from scale thrust.

Normal thrust. - Normal thrust is the theoretical thrust that would be obtained with the engine and the standard-engine tail pipe equipped with a nozzle of a size that gives the same turbine-outlet pressures and temperatures as were encountered with tail-pipe burning under the same flight conditions. Such a definition of normal thrust takes into account engine deterioration. The normal thrust of the engine was calculated from measurements during the tail-pipe burning program of total pressure and temperature at the turbine outlet, gas flow at the turbine outlet, and from previously determined total-pressure loss ratio across the standard-engine tail pipe.

$$F_{n,e} = \frac{W_{g,6}}{g} C_J \sqrt{\frac{2\gamma_6}{\gamma_6 - 1} gRt_6 \left[\left(\frac{P_8'}{P_0}\right)^{\frac{\gamma_6 - 1}{\gamma_6}} - 1\right]} - \frac{W_{a,1}}{g} V_0$$ (14)

Experimental data indicated that the total-pressure loss through the standard-engine tail pipe from station 6 to station 8 at rated engine speed was nearly 0.032 P_6; P_8' is therefore equal to approximately 0.968 P_6. The jet velocity coefficient C_J used in equation (14) is shown as a function of tail-pipe pressure ratio:

1372

Exhaust-nozzle pressure ratio, P_8/p_0
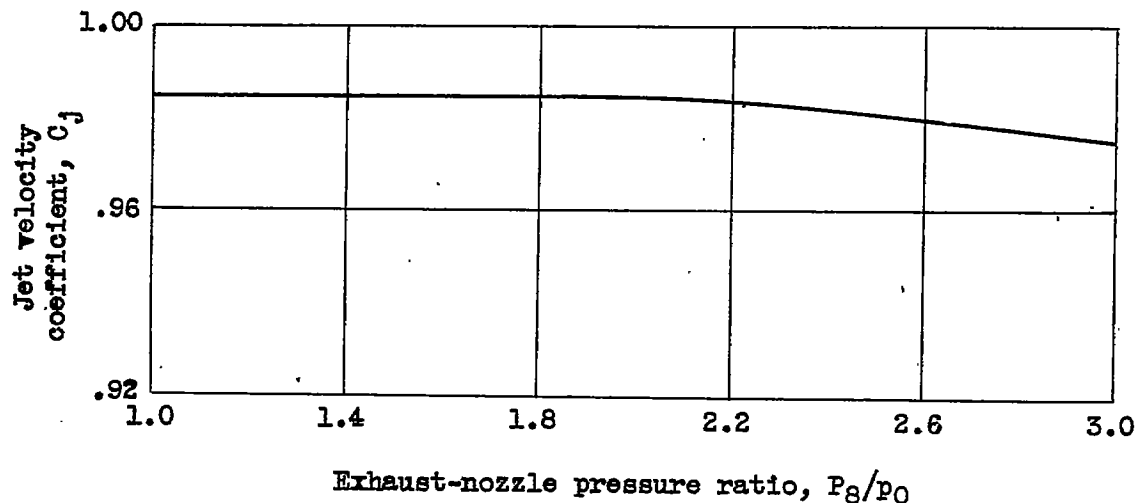
Augmented thrust ratio is defined as:

$$\frac{\text{Scale net thrust, } F_{n,s}}{\text{Normal engine thrust, } F_{n,e}}$$

As previously stated, for the normal thrust, $P_8{}'$ was approximately equal to $0.968\ P_6$. Experimental data also showed that with the tail-pipe burner inoperative, P_8 was approximately equal to $0.942\ P_6$. This thrust ratio was calculated as follows:

$$\frac{F_n{}^*}{F_{n,e}} = \frac{C_J \dfrac{W_{g,6}}{g} \sqrt{\dfrac{2\gamma_6}{\gamma_6-1}\, gRT_6 \left[1-\left(1.061\ \dfrac{p_0}{P_6}\right)^{\frac{\gamma_6-1}{\gamma_6}}\right]} - \dfrac{W_{a,1}}{g} V_0}{C_J \dfrac{W_{g,6}}{g} \sqrt{\dfrac{2\gamma_6}{\gamma_6-1}\, gRT_6 \left[1-\left(1.033\ \dfrac{p_0}{P_6}\right)^{\frac{\gamma_6-1}{\gamma_6}}\right]} - \dfrac{W_{a,1}}{g} V_0} \tag{15}$$

where $F_n{}^*$ is the thrust with tail-pipe burner inoperative. At all flight Mach numbers, T_6 was assumed a value of 1700° R. For various flight Mach numbers, P_6/p_0 and V_0 were obtained from tail-pipe burning data. The jet velocity coefficients were assumed to be equal for both configurations.

1372

Exhaust-gas total temperature. - The total temperature of the exhaust gas was calculated from the thrust equation and is based on rake thrust.

$$T_9 = \frac{(\gamma_8 - 1)g(F_{j,8})^2}{2\gamma_8 R(W_{g,8})^2 \left[1 - \left(\frac{p_0}{P_8}\right)^{\frac{\gamma_8 - 1}{\gamma_8}}\right]} \tag{16}$$

REFERENCES

1. Conrad, E. William, and Prince, William R.: Altitude Performance and Operational Characteristics of 29-Inch-Diameter Tail-Pipe Burner with Several Fuel Systems and Flame Holders on J35 Turbojet Engine. NACA RM E9G08, 1949.

2. Thorman, H. Carl, and Campbell, Carl E.: Altitude-Wind-Tunnel Investigation of Tail-Pipe Burner with Converging Conical Burner Section on J35-A-5 Turbojet Engine. NACA RM E9I16, 1950.

3. Golladay, Richard L., and Bloomer, Harry E.: Altitude Performance and Operational Characteristics of 29-Inch-Diameter Tail-Burner with Several Fuel Systems and Fuel-Cooled Stage-Type Flame Holders on J35-A-5 Turbojet Engine. NACA RM E50A19, 1950.

4. Fleming, William A., and Wallner, Lewis E.: Altitude-Wind-Tunnel Investigation of Tail-Pipe Burning with a Westinghouse X24C-4B Axial-Flow Turbojet Engine. NACA RM E8J25e, 1948.

5. Wallner, Lewis E., and Fleming, William A.: Reynolds Number Effect on Axial-Flow Compressor Performance. NACA RM E9G11, 1949.

6. Turner, Richard L., and Lord, Albert M.: Thermodynamic Charts for the Computation of Combustion and Mixture Temperatures at Constant Pressure. NACA TN 1086, 1946.

1372

19

CONFIDENTIAL

TABLE I – PERFORMANCE DATA WITH TAIL-PIPE BURNER

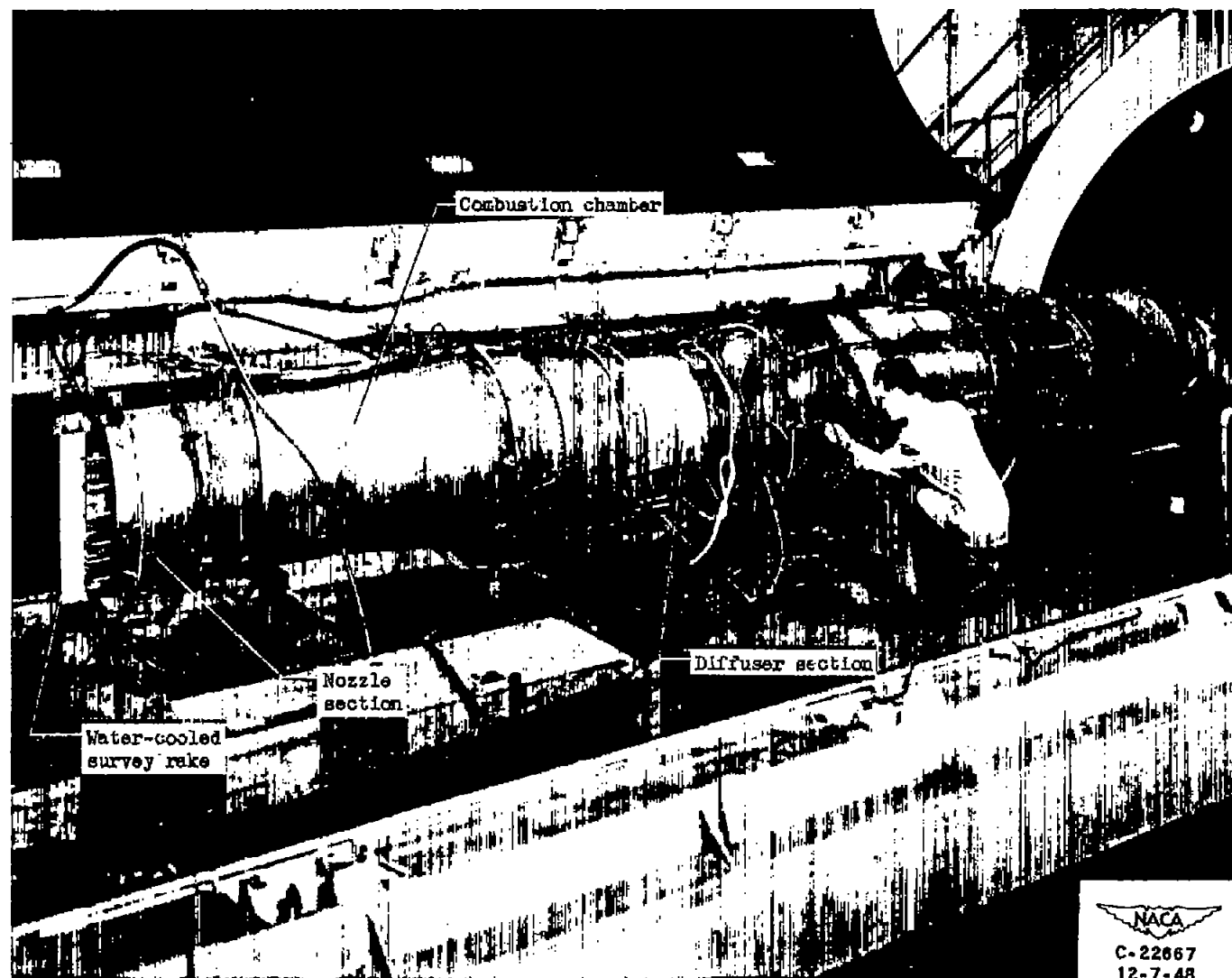| Run	Altitude (ft)	Flight Mach number M_0	Ambient static pressure p_0 (lb/sq ft abs.)	Engine inlet Total pressure P_1 (lb/sq ft abs.)	Engine inlet Total temperature T_1 (°R)	Engine fuel flow $W_{f,e}$ (lb/hr)	Tail-pipe fuel flow $W_{f,t}$ (lb/hr)	Tail-pipe fuel distribution Primary system	Tail-pipe fuel distribution Secondary system	Scale thrust Jet (lb)	Scale thrust Net (lb)	Engine-inlet air flow $W_{a,1}$ (lb/sec)	Specific fuel consumption W_f/F_n (lb/(hr)(lb thrust))	Total fuel-air ratio f/a	Tail-pipe fuel-air ratio $(f/a)_t$	Tail-pipe combustion efficiency $\eta_{b,t}$	Tail-pipe burner inlet Total pressure P_5 (lb/sq ft abs.)	Tail-pipe burner inlet Total temperature T_5 (°R)	Combustion chamber-inlet velocity V_7 (ft/sec)	Exhaust nozzle Total pressure P_8 (lb/sq ft abs.)	Exhaust nozzle Total temperature T_9 (°R)
1	15,000	0.225	1186	1250	501	3350	7430	0.33	0.67	4115	3675	56.92	2.931	0.0557	0.0493	0.854	2265	1679	535	1925	3410
2	15,000	.235	1183	1250	495	3160	6400	.34	.66	3830	3371	57.28	2.834	.0472	.0413	.845	2176	1602	535	1858	3112
3	15,000	.225	1191	1235	502	3000	5500	.35	.65	3520	3077	57.12	2.762	.0421	.0360	.857	2111	1565	538	1805	2917
4	15,000	.225	1186	1230	499	2710	4720	.37	.63	3057	2617	57.03	2.840	.0568	.0393	.721	1994	1463	532	1704	2480
5	15,000	.230	1190	1235	503	2200	3680	.41	.59	1752	1302	57.18	4.615	.0291	.0217	.116	1708	1303	572	1475	1418
6	25,000	.225	781	810	492	2190	5000	.36	.64	2718	2430	37.62	2.959	.0541	.0499	.805	1477	1676	525	1261	3312
7	25,000	.225	785	814	491	2160	4780	.37	.63	2706	2415	37.99	2.874	.0517	.0467	.812	1471	1648	523	1258	3232
8	25,000	.225	781	809	497	2060	4650	.39	.61	2461	2176	37.37	2.901	.0477	.0419	.813	1424	1633	527	1216	3080
9	25,000	.225	778	805	500	1930	3680	.41	.59	2217	1937	37.10	2.897	.0427	.0359	.774	1362	1562	524	1164	2812
10	25,000	.215	785	810	495	1900	3260	.42	.58	2104	1834	37.73	2.813	.0386	.0310	.711	1349	1520	537	1138	2541
11	25,000	.535	781	948	501	2620	7200	.33	.67	3777	2993	44.34	3.280	.0637	.0614	.733	1765	1697	527	1500	3466
12	25,000	.540	778	945	495	2540	6800	.34	.66	3559	2763	44.01	3.161	.0562	.0528	.784	1708	1665	530	1456	3351
13	25,000	.540	777	944	496	2470	5500	.35	.65	3384	2609	43.91	3.053	.0514	.0466	.846	1681	1624	541	1432	3298
14	25,000	.530	781	946	499	2340	4690	.37	.63	3099	2324	44.14	3.023	.0451	.0388	.836	1625	1574	546	1376	3012
15	25,000	.535	782	949	505	1760	3470	.41	.59	1934	1151	44.13	4.841	.0356	.0288	.309	1359	1364	588	1109	1746
16	25,000	.745	781	1159	489	3100	7300	.33	.67	4893	3605	54.44	2.897	.0645	.0502	.776	2072	1647	531	1756	3262
17	25,000	.755	781	1140	496	2800	6000	.34	.66	4486	3186	53.61	2.762	.0466	.0409	.823	1965	1564	528	1668	3050
18	25,000	.770	773	1140	492	2540	4870	.36	.64	3975	2665	53.55	2.782	.0392	.0325	.763	1853	1472	543	1537	2813
19	25,000	.755	780	1159	496	2400	4500	.38	.62	3605	2311	53.27	2.986	.0367	.0296	.731	1797	1424	539	1458	2472
20	25,000	.755	778	1133	495	2230	4170	.39	.61	3376	2092	53.07	3.059	.0341	.0271	.590	1708	1376	551	1392	2163
21	25,000	.765	774	1136	498	2000	3780	.40	.60	2602	1294	53.40	4.468	.0306	.0238	.295	1533	1501	603	1234	1839
22	25,000	.765	778	1143	502	1890	2500	.46	.54	1894	576	53.50	7.620	.0232	.0155	~.104	1426	1240	675	1083	1128
23	35,000	.235	494	514	496	1450	3550	.41	.59	1718	1527	23.78	3.271	.0593	.0588	.689	936	1716	544	800	3267
24	35,000	.225	493	511	497	1410	3000	.43	.57	1625	1444	23.44	3.053	.0551	.0484	.768	921	1707	552	781	3215
25	35,000	.225	493	511	497	1380	2700	.45	.55	1552	1371	23.44	2.975	.0491	.0433	.833	914	1696	552	776	3182
26	35,000	.225	496	514	496	1340	2400	.46	.54	1346	1167	23.52	3.119	.0457	.0370	.665	853	1595	551	730	2662
27	35,000	.225	494	512	498	1300	2100	.48	.52	1297	1116	23.53	2.957	.0394	.0319	.665	847	1584	562	714	2509
28	45,000	.235	306	318	493	880	2100	.48	.52	975	860	14.55	3.465	.0679	.0550	.600	557	1713	558	477	3014
29	45,000	.225	308	319	491	870	1900	.50	.50	902	792	14.56	3.498	.0636	.0494	.554	550	1718	570	463	2796
30	45,000	.235	306	318	493	860	1800	.50	.50	878	763	14.55	3.488	.0517	.0467	.546	543	1716	577	457	2783
31	45,000	.240	303	315	490	840	1750	.50	.50	894	778	14.51	3.330	.0505	.0454	.582	545	1707	570	459	2752
32	45,000	.225	301	312	494	810	1700	.51	.49	824	715	14.17	3.510	.0501	.0447	.481	522	1697	576	458	2545
33	45,000	.220	299	309	492	800	1660	.51	.49	808	701	13.96	3.510	.0498	.0444	.552	517	1677	569	436	2671
34	45,000	.205	299	308	495	790	1600	.52	.48	794	697	13.87	3.431	.0497	.0450	.661	530	1666	546	443	2645

NACA

Figure 1. - Installation of engine and tail-pipe burner in altitude wind tunnel.
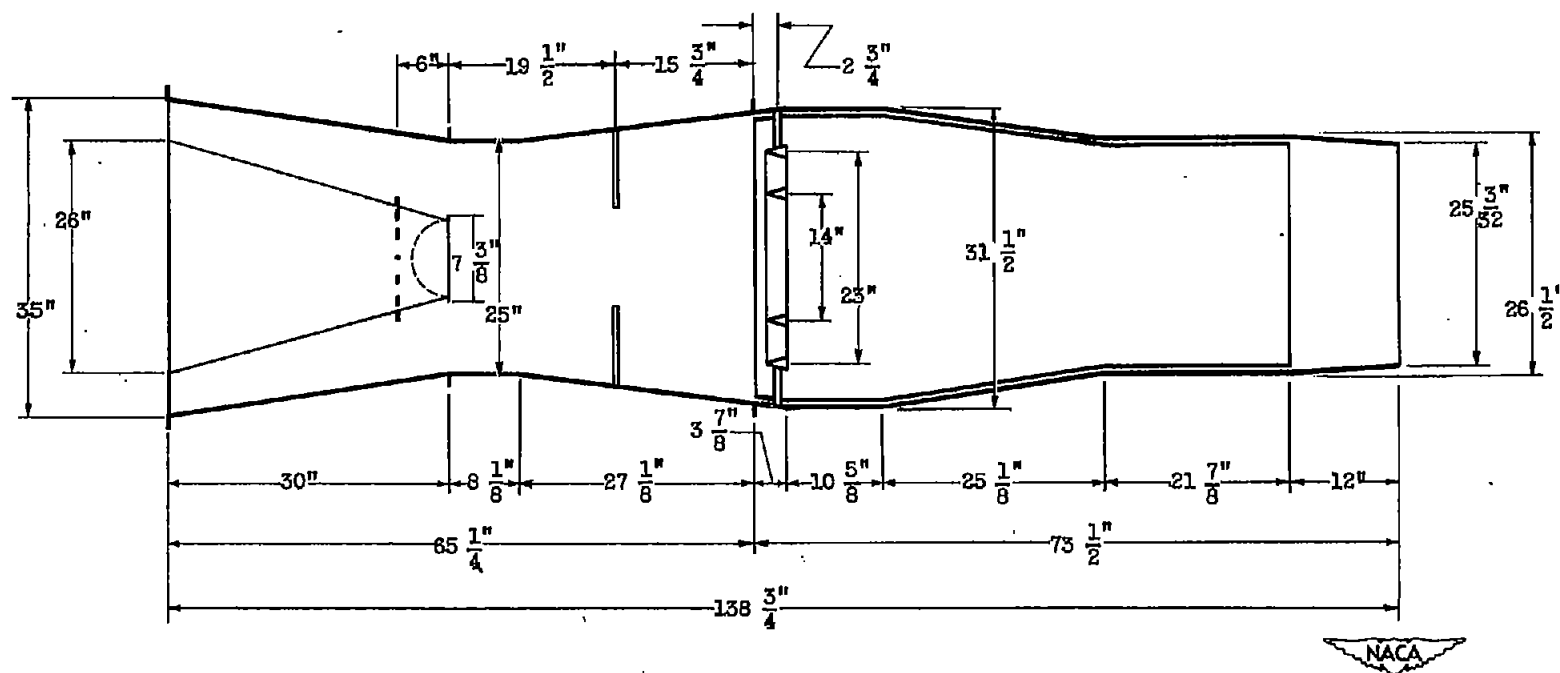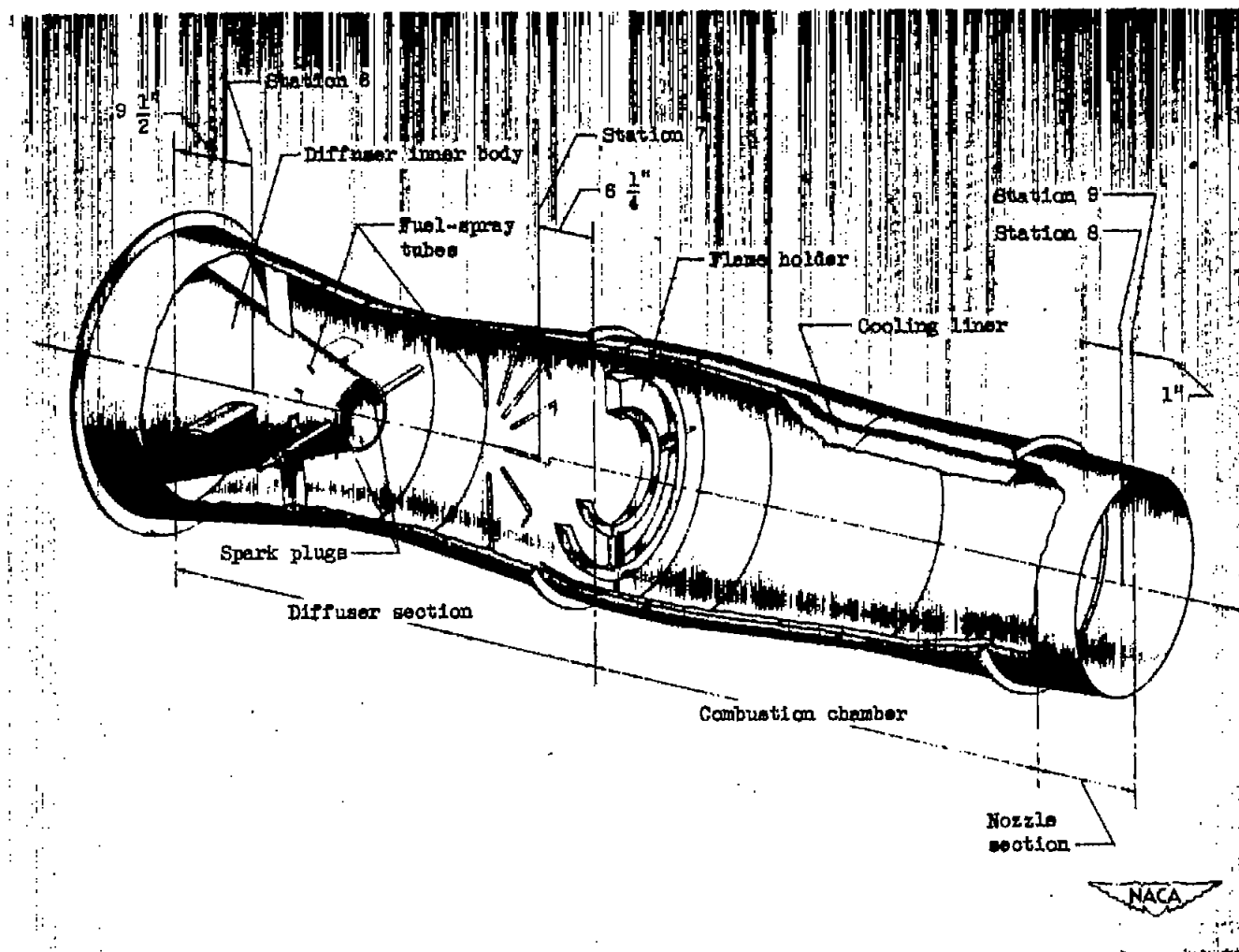
Figure 2. - Cross-sectional view of tail-pipe burner.
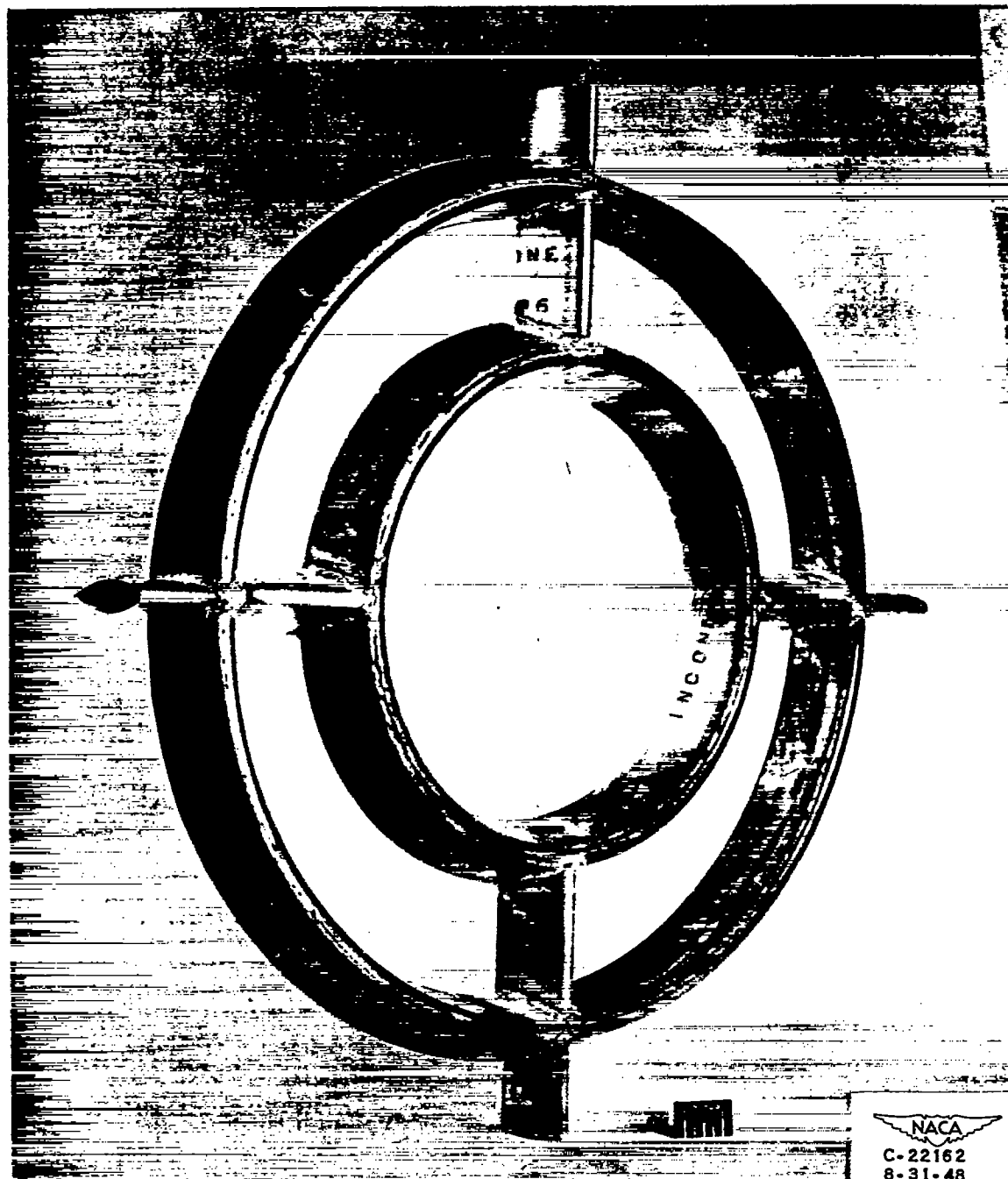
Figure 3. - Schematic diagram of tail-pipe burner.

1372

Figure 4. - Typical two-annular V-type flame holder.

Detail A: four holes per
tube, 0.031-inch diameter;
fuel spray perpendicular
to gas flow.

$2\frac{5}{16}$"

$4\frac{13}{16}$"

$7\frac{5}{16}$"

Detail A

$18\frac{1}{2}$ inches upstream
of flame holder

Detail B: two holes per
tube, 0.031-inch diameter;
fuel spray perpendicular
to gas flow.

1" $1\frac{3}{16}$"

Detail B

44 inches upstream
of flame holder

Breeze flow meter

Hydraulic
throttle

Fuel
supply

Solenoid
valve

Rotameter

Pilot cone nozzle

Primary system

Solenoid
valve

Flow divider

Pressure gages

Atmospheric vent

Secondary system

Detail C: six holes per
tube, 0.041-inch diameter;
fuel spray perpendicular
to gas flow.

$1\frac{5}{8}$"

3"

$8\frac{1}{2}$"

$3\frac{5}{8}$"

Detail C

Breeze
flow meter

$18\frac{1}{2}$ inches upstream
of flame holder

NACA

Figure 5. - Schematic diagram of tail-pipe fuel system for configuration C.
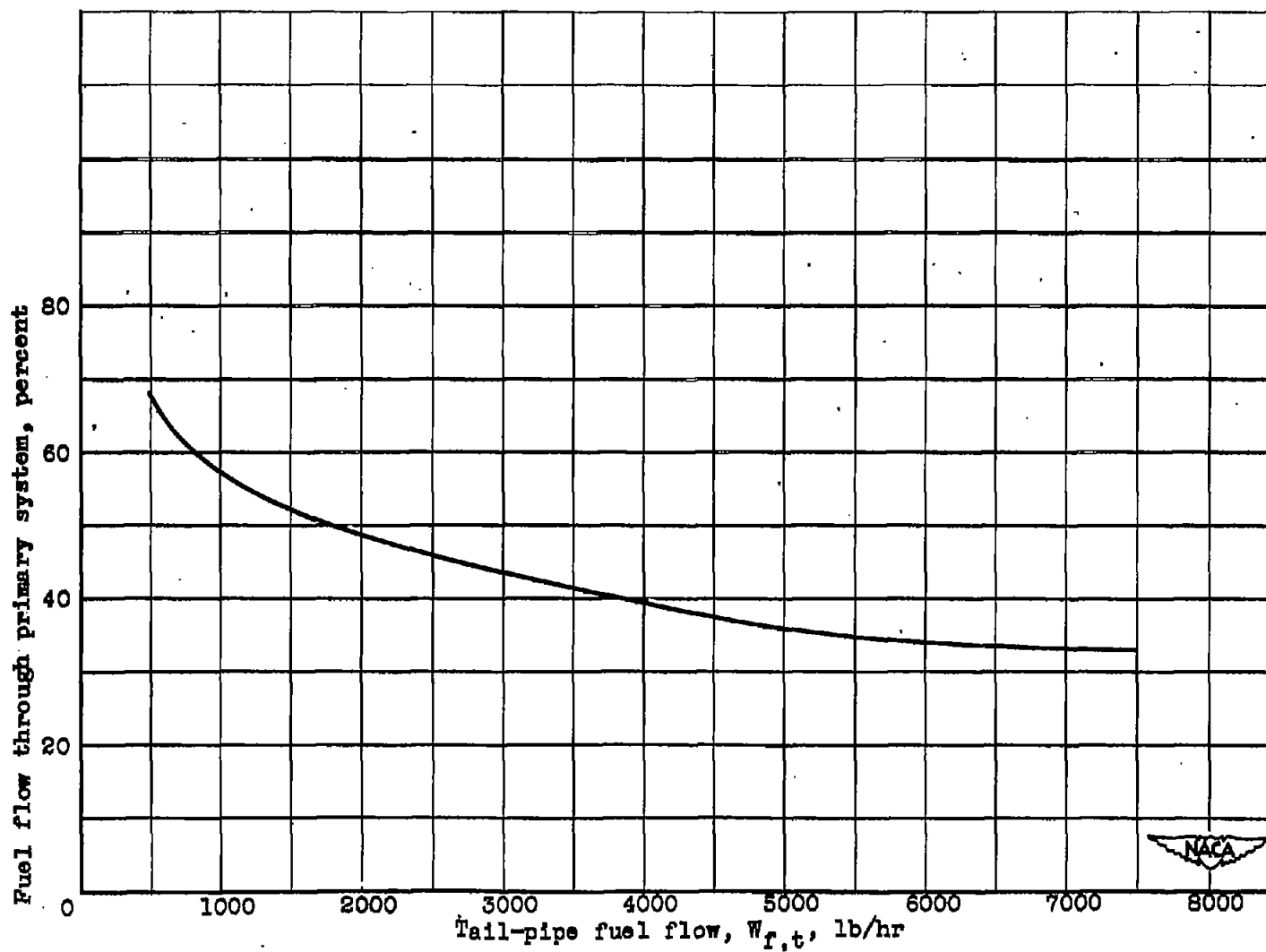
Figure 6. – Flow divider schedule for tail-pipe burner.

CONFIDENTIAL

1372

O   Total-pressure tube
●   Static-pressure wall orifice
X   Thermocouple
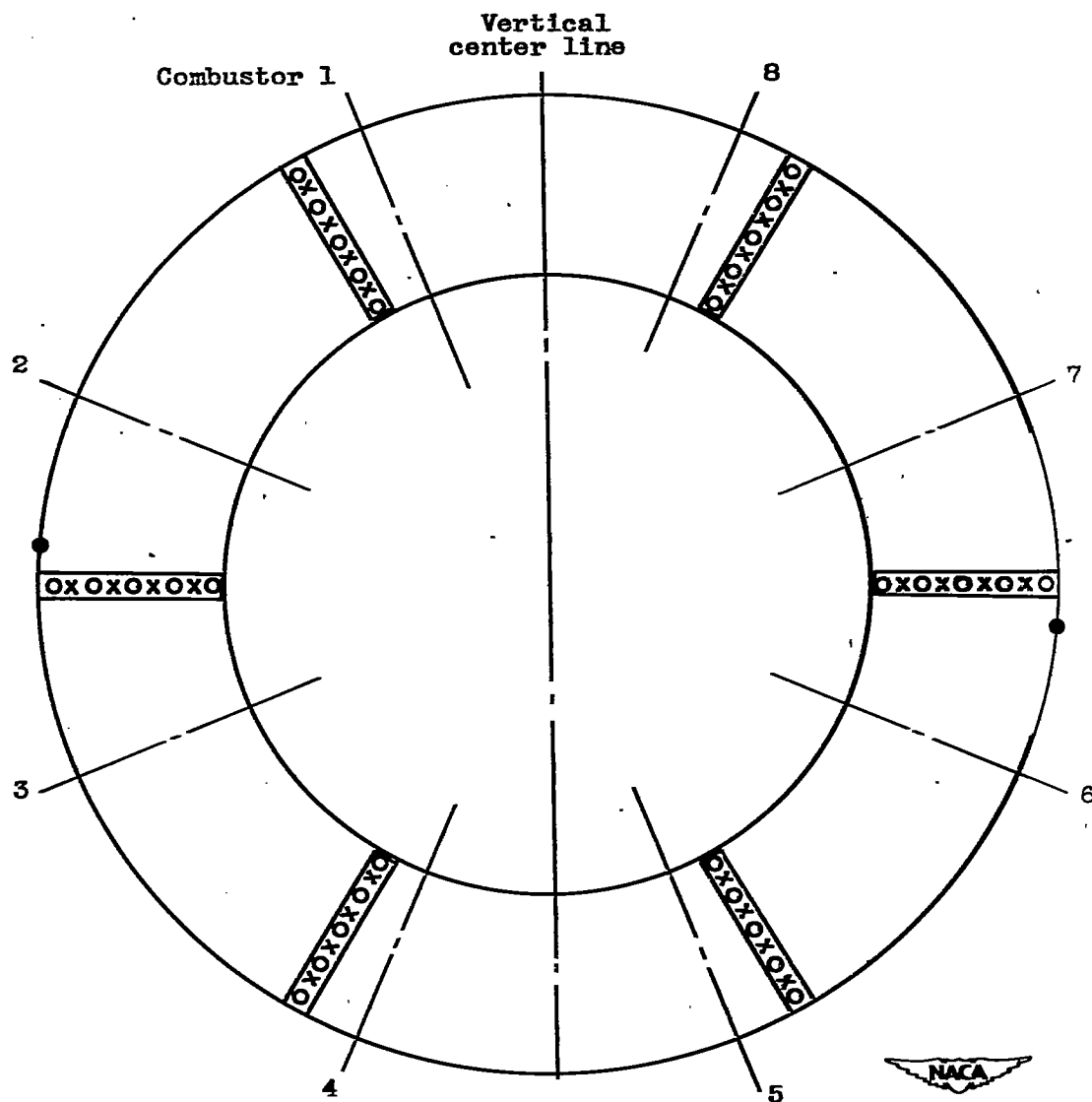
(a) Tail-pipe-burner inlet, station 6, $9\frac{1}{2}$ inches downstream of tail-
pipe-burner inlet.

Figure 7. – Cross sections of measuring stations showing location of
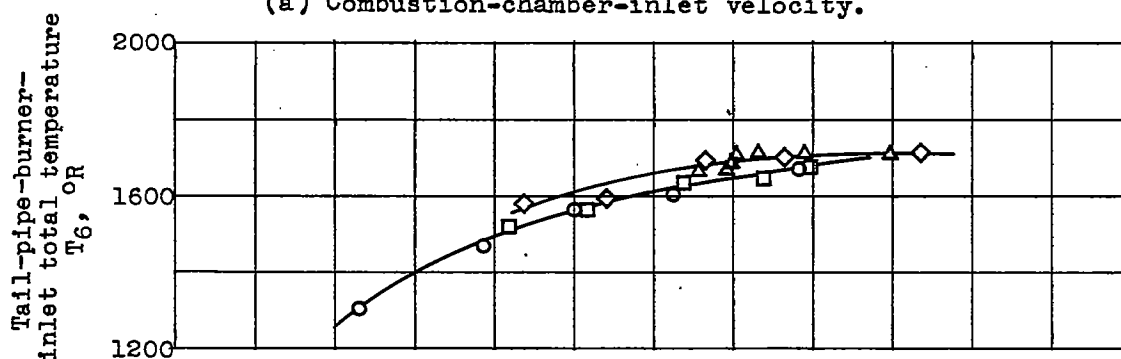instrumentation. Viewed from upstream.

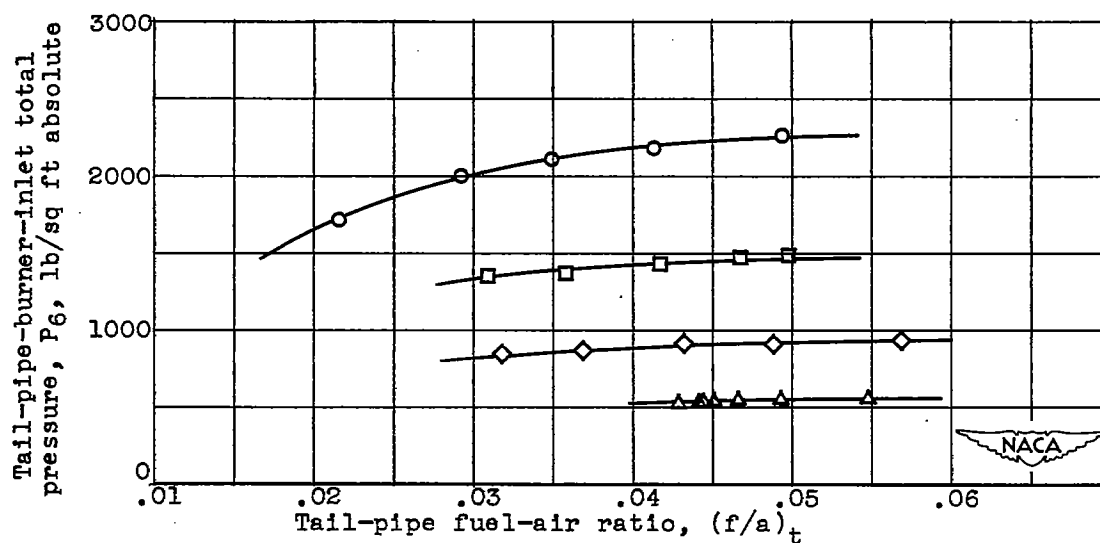CONFIDENTIAL
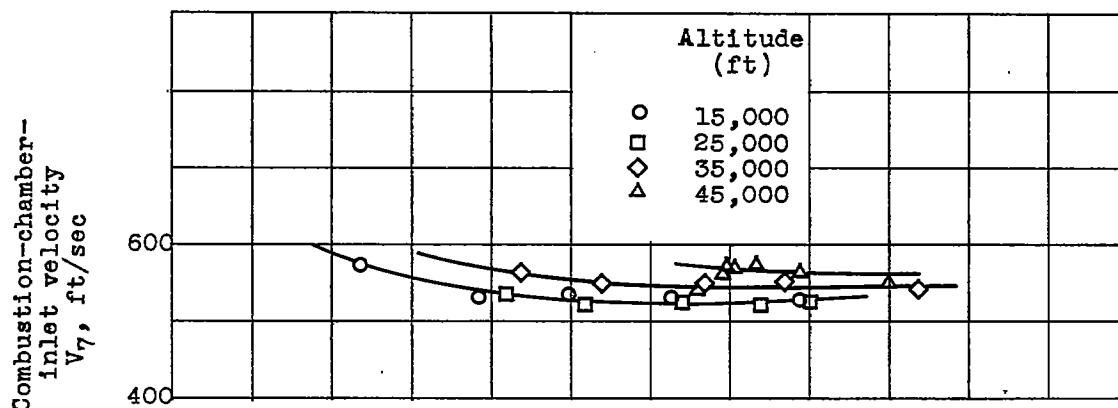
CONFIDENTIAL

O Total-pressure tube
● Static-pressure tube
x Thermocouple

(b) Exhaust nozzle, station 8, 1 inch upstream of exhaust-
nozzle outlet.

Figure 7. – Concluded. Cross sections of measuring stations
showing location of instrumentation. Viewed from upstream.

1372

(a) Combustion-chamber-inlet velocity.

(b) Tail-pipe-burner-inlet temperature.

(c) Tail-pipe-burner-inlet pressure.

Figure 8. – Effect of altitude on variation of combustion-chamber-inlet
velocity and tail-pipe-burner-inlet conditions with tail-pipe fuel-
air ratio. Engine speed, 7900 rpm; flight Mach number, 0.23.
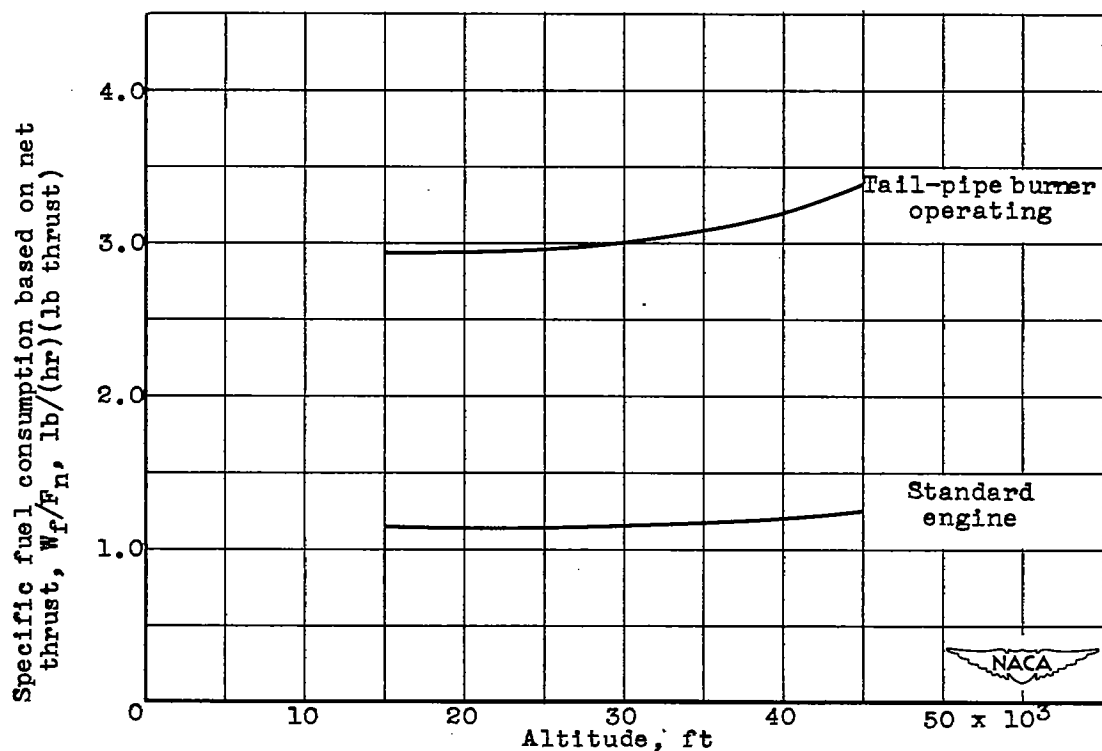
1372
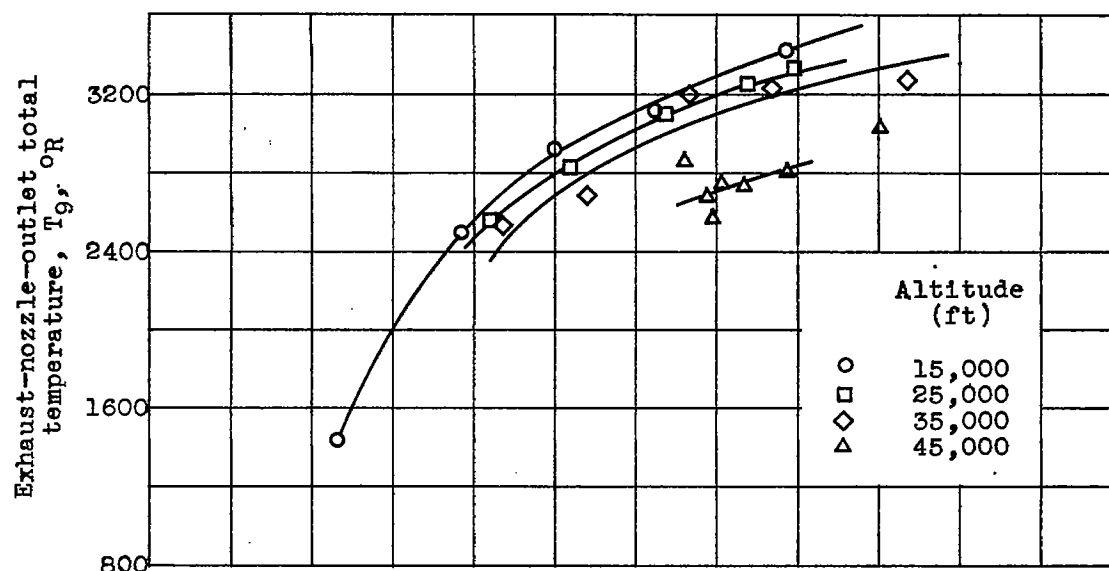
(a) Exhaust-gas total temperature.
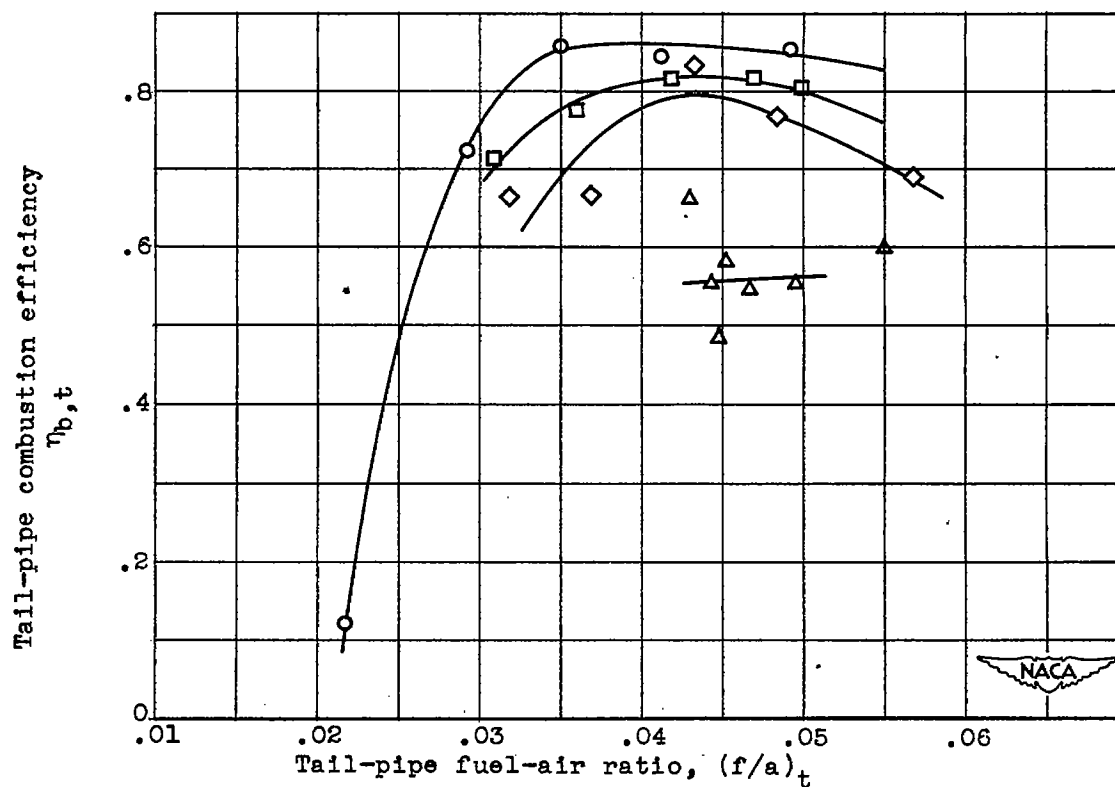
(b) Tail-pipe combustion efficiency.

Figure 9. – Effect of altitude on variation of exhaust-gas tempera-
ture and tail-pipe combustion efficiency with tail-pipe fuel-air
ratio.　Flight Mach number, 0.23; engine speed, 7900 rpm.
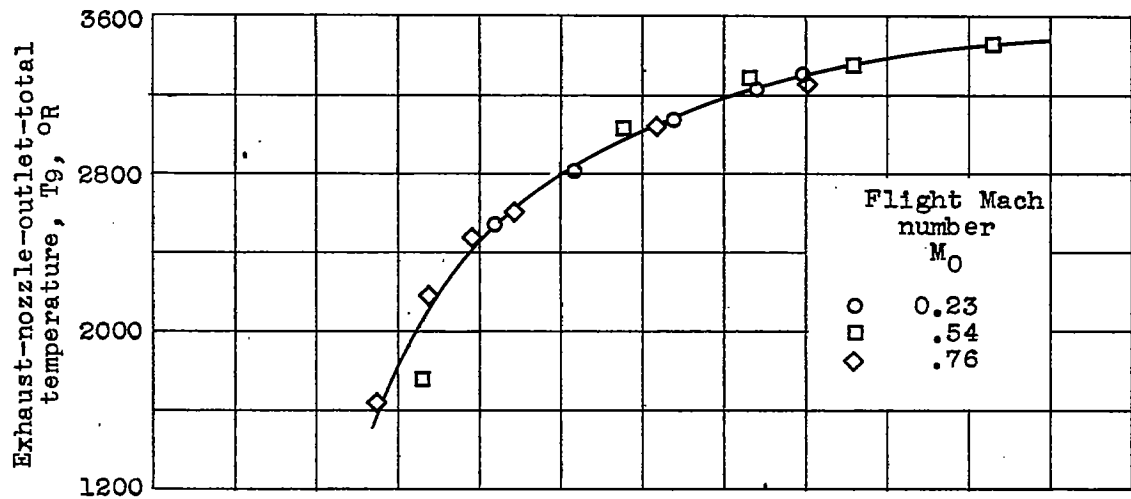
1372

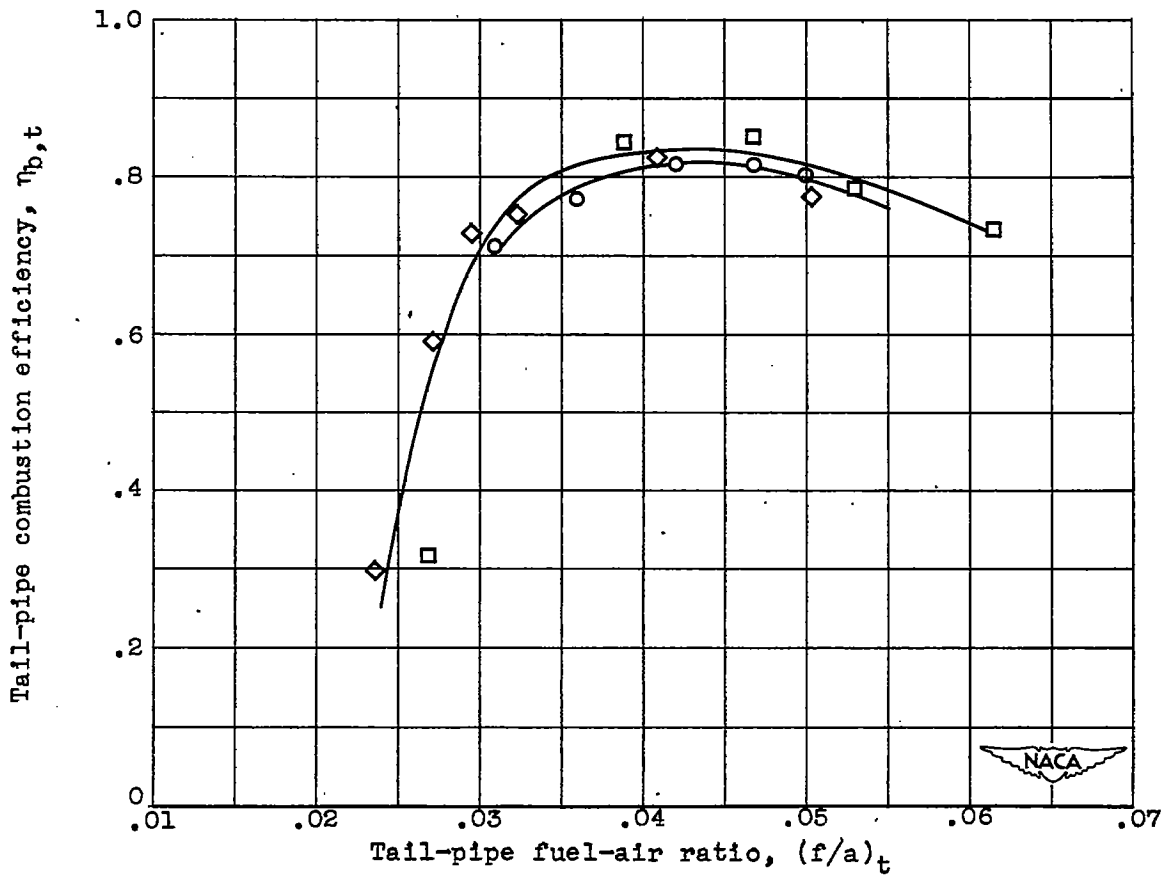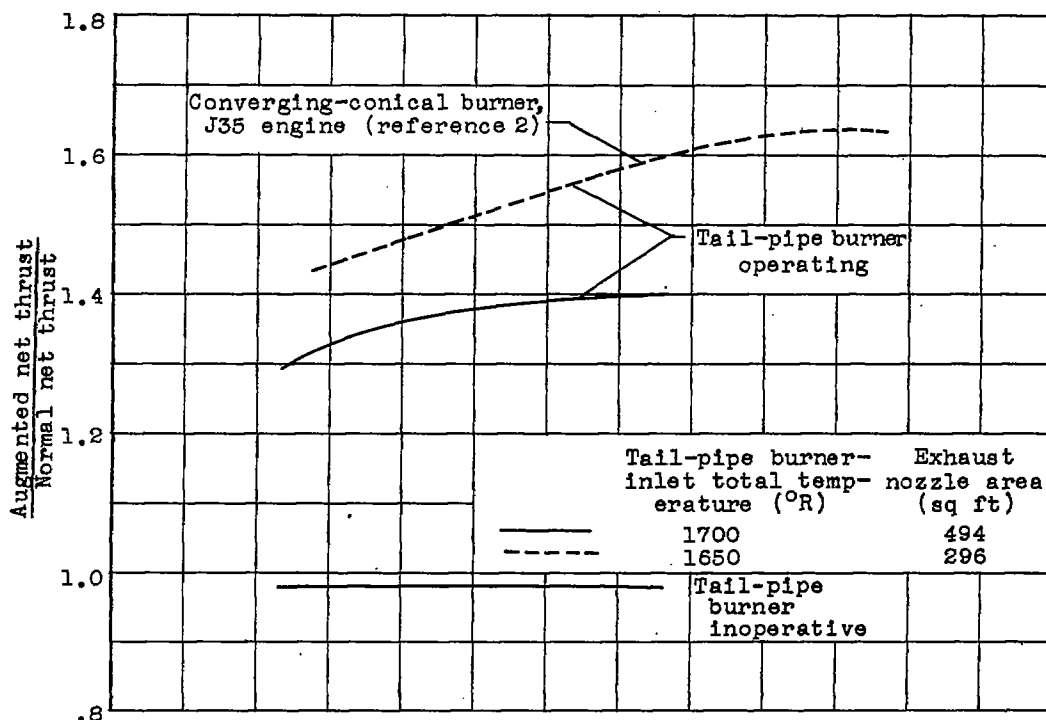(a) Augmented thrust ratio.

(b) Specific fuel consumption.

Figure 10. – Variation of over-all burner performance characteristics with altitude. Tail-pipe burner-inlet temperature, 1700 ^{o}R; Mach number, 0.23; exhaust-nozzle-outlet area, 494 square inches; engine speed, 7900 rpm.

1372

(a) Combustion-chamber-inlet velocity.

(b) Tail-pipe burner inlet temperature.

(c) Tail-pipe-burner-inlet pressure.

Figure 11. – Effect of flight Mach number on variation of combustion-chamber-inlet velocity and tail-pipe-burner-inlet conditions with tail-pipe fuel-air ratio. Altitude, 25,000 feet; engine speed, 7900 rpm.

1372

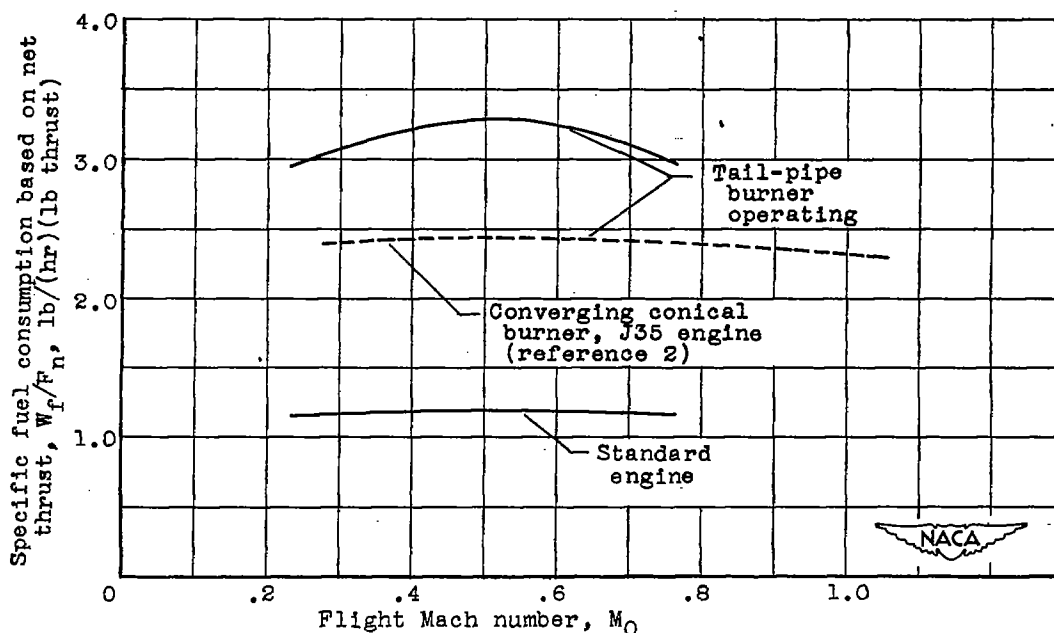(a) Exhaust-gas total temperature.

(b) Tail-pipe combustion efficiency.

Figure 12. – Effect of flight Mach number on variation of exhaust-gas
temperature and tail-pipe combustion efficiency with tail-pipe
fuel-air ratio. Altitude, 25,000 feet; engine speed, 7900 rpm.

CONFIDENTIAL

1372

(a) Augmented thrust ratio.

(b) specific fuel consumption.

Figure 13. — Variation of over-all burner performance characteristics with flight Mach number. Altitude, 25,000 feet; engine speed, 7900 rpm.

CONFIDENTIAL